WAVE-RELATED TRANSPORT AND NEARSHORE MORPHOLOGY

Leo van Rijn[1], Gerben Ruessink[1], Bart Grasmeijer[1],
Jebbe van der Werf[2], Jan Ribberink[2]

1. Department of Physical Geography, University of Utrecht. The Netherlands.
   leo.vanrijn@wldelft.nl; g.ruessink@geo.uu.nl; b.grasmeijer@alkyon.nl
2 Department of Civil Engineering, University of Twente. The Netherlands.
   j.j.vanderwerf@ctw.utwente.nl; j.s.ribberink@ctw.utwente.nl

Abstract: This paper discusses the simulation of nearshore bar migration using the CROSMOR profile model. Two sediment transport formulations have been used : the method of Van Rijn (2006) and that of Van der Werf (2006). The model has been applied to two large-scale laboratory experiments in the Delta flume of Delft Hydraulics. Both transport models can represent the trends observed in the laboratory experiments.

INTRODUCTION

As surface gravity waves arrive at the shore from deep water, they transfrom primarily owing to shoaling, refraction, breaking, and non-linear wave interactions. These interactions cause dramatic transformations of the wave shape. From deep into intermediate waterdepths, the initially symmetric, nearly sinusoidal profiles develop into profiles with sharp crests and broad, flat troughs. This horizontal aymmetry is known as skewness. Into shallower water, the waves ultimately transform into pitched-forward, sawtooth profiles, known as (vertical) asymmetry, which have zero-skewness. Field studies, like those of Doering and Bowen (1995), have indicated that near-bed velocity skewness and asymmetry can be parameterized reasonably well with the local Ursell number, suggesting that wave non-linearity is determined locally, and does not depend on, for instance, beach slope. The mechanism for the wave shape transformation is nonlinear, near-reasonant triad interactions, involving the energy transfer from two primary waves with frequencies ω_1 and ω_2 to a secondary wave with frequency $\omega_1 + \omega_2$. This secondary wave is phase locked to the primary waves, initially with a phase difference of 0 degrees to result in a skewed wave profile, increasing to -90 degrees for a sawtooth wave.

The local non-linearity of the near-bed orbital motion is important to sediment transport. The recognition that skewed waves may induce onshore transport because of the much larger onshore than offshore velocities already dates back to the 19th century. The relevance of asymmetric waves to onshore transport (e.g., Hoefel and Elgar, 2003) is still under considerable debate (e.g., Henderson et al., 2004; Hsu et al., 2006). However, the notion that wave non-linearity leads to onshore transport only may be too simple. Fundamentally different physical processes determine sand transport rates above plane and rippled sand beds in oscillatory flow. Above plane beds, momentum transfer and associated sediment dynamics occurs primarily by turbulent diffusion. In contrast, in the bottom part of the boundary layer above rippled beds, momentum transfer and the associated sediment dynamics are dominated by coherent periodic vortex structures; above this, in a layer of thickness of about 1-2 ripple heights, the coherent motions break down and are replaced by random turbulence. The effect of this is that sand is entrained into suspension to considerably greater heights above rippled beds than above plane beds. In addition, the phase of sand pick-up from the bottom during the wave-cycle is also significantly different above rippled beds, with pick-up being linked to the phase of vortex shedding. This has potentially important consequences for the net sand transport rate beneath asymmetrical waves, which can be in the negative ('offshore') direction despite the larger positive ('onshore') orbital velocities (Van der Werf, 2006). The aim of the present paper is to present preliminary work on the influence of bedforms, wave shape and phase-lags on wave-induced suspended sediment transport. Existing engineering transport formulations for wave-induced suspended sediment transport, like those of Houwman and Ruessink (1996), are reviewed and adjusted to incorporate phenomena like phase lags. We then incorporate the various formulations in the CROSMOR profile model and apply it to the prediction of sandbar migration in two large-scale laboratory tests. The CROSMOR model has been described earlier by the first author. Papers on the CROSMOR-model can be downloaded from www.leovanrijn-sediment.com.

CROSS-SHORE TRANSPORT PROCESSES

In recent years, many full-scale oscillatory flow tunnel experiments have been carried out in order to increase the insight of the complex nature of cross-shore sediment transport and to obtain reliable data for validation and further development of various types of models. One of the advantages of those type of experiments is that net sediment transport rates can be measured accurately. Figure 1 shows measured net sediment transport rates as a function of the mobility number $\psi=2(u_{rms})^2/((s-1)gd_{50})$, with u_{rms} =the root-mean-square orbital velocity, s=the relative sediment density, g =the acceleration due to gravity and d_{50} =the median grain-size (Van der Werf, 2006). The orbital flow was regular asymmetric with larger positive (‘onshore’) velocities and smaller negative (‘offshore’) velocities and the degree of flow asymmetry was similar across the experiments.

This figure shows that the net sediment transport rate is alternately negative (‘offshore-directed’) and positive (‘onshore-directed’), depending on presence or absence of ripples and the grain-size. For mobility numbers smaller than 100, the bed is covered with two-dimensional ripples. On the lee-side of these ripples vortices are generated, which are

ejected at times of flow reversal. As a consequence, there exists strong phase differences between the peak concentrations and peak velocities. Van der Werf (2006) shows that this results in negative net wave-induced sediment transport when suspension is dominant.

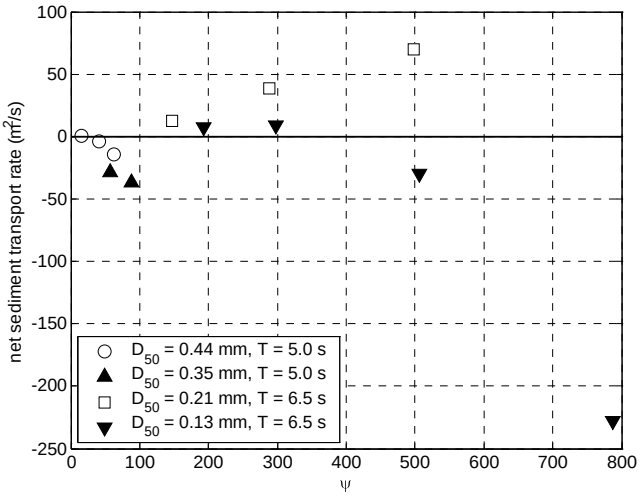

Fig. 1. Net sediment transport rates as function of mobility parameter

For larger mobility numbers, the ripples are washed out, the bed becomes plane again and the sheet-flow regime is entered. Sediment is transported in a thin layer of a few centimetres thick close to the bed. Experimental results show that net sediment transport rates mostly are in the 'onshore' direction in the sheet-flow regime, because the sediment responds almost instantaneously to the flow. However, phase lags between velocity and concentration (delayed pick-up and settling) become also important in the sheet-flow regime for finer sediments. When phase lags are important, the net sediment transport in oscillatory flow cannot be modelled in a quasi-steady way, and better agreement with the observed transport data may be obtained with the semi-unsteady transport model of Dohmen-Janssen (1999). Grasmeijer (2002) has found that the net wave-related suspended transport under irregular waves over a rippled bed in a large-scale laboratory flume (Delta flume of Delft Hydraulics) and at a field site (Egmond beach, The Netherlands) always is onshore-directed.

Figure 2 shows the schematic behaviour of the net sediment transport rate as a function of the Shields mobility parameter (θ') with: $\theta' = \tau'_{b,w}/((\rho_s-\rho_w)gd_{50})$; $\tau'_{b,w}$ = *wave-related bed shear stress*. In the ripple regime the net sand transport under low waves (mobility parameter $\theta'<1$) may become negative (in offshore direction) depending on the shape and dimensions of the ripples and the type of oscillatory flow (regular of irregular wave motion), (Van der Werf, 2006). For mobility parameters approaching 1 ($\theta' \cong 1$) the ripples will be washed out (sheet flow regime) and the net transport rate will become positive again. For very large mobility parameters ($\theta' \cong 5$ to 10) the net transport rate may become very small again due to the generation of phase lags between velocity and concentrations in the sheet flow layer (U_w=1.3 m/s, T=4 s and d_{50}=0.13 mm, see Dohmen-Janssen, 1999). Accurate modelling of wave-induced cross-shore transport and

nearshore morphology using a profile model thus requires an accurate modelling of the shape of the near-bed orbital flow and the bed form regime.

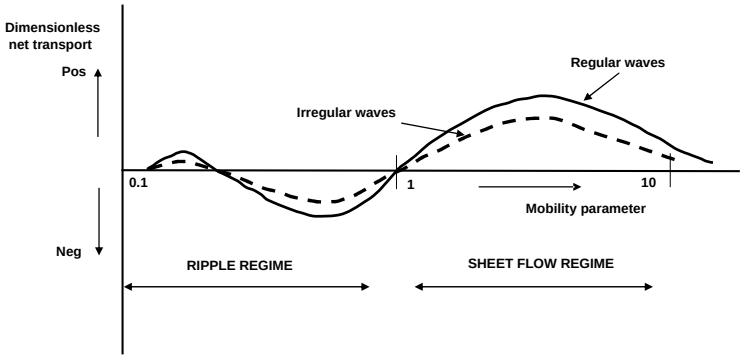

Fig. 2. Schematic behaviour of net sand transport rates (dimensionless) as function of grain-related mobility parameter

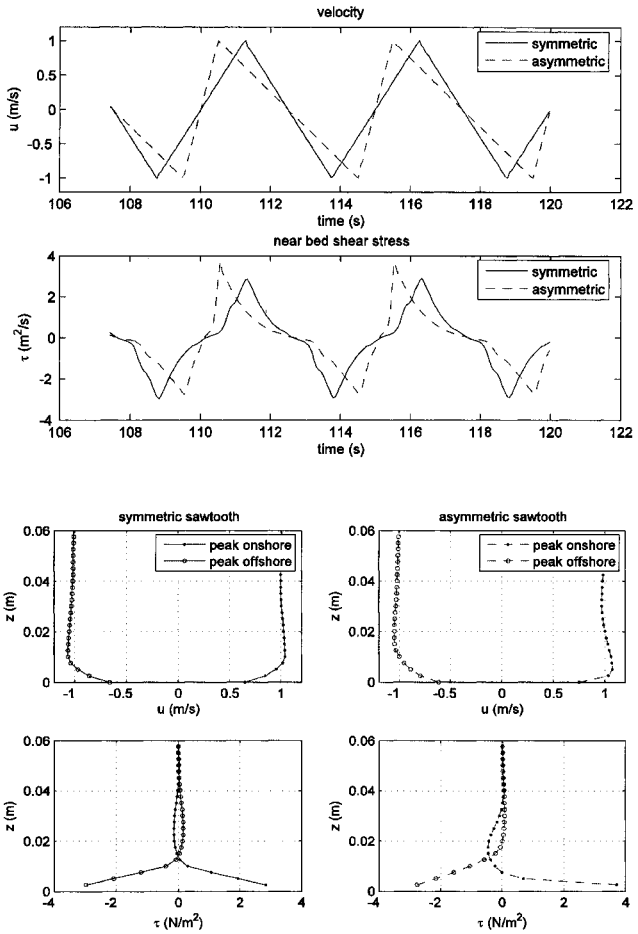

Fig. 3. Peak onshore and offshore velocities and bed-shear stresses in the case of symmetric and asymmetric saw-tooth waves

MODELLING OF BED-SHEAR STRESSES IN ASYMMETRIC WAVE MOTION

The peak orbital velocities in the CROSMOR model are computed by using the method of Isobe-Horikawa (1982), as modified by Grasmeijer (2002). This method can represent the skewness effect, but not the asymmetry effect under forward-leaning waves. In sinusoidal wave motion over a flat bed the instantaneous bed-shear stress is described as:

$$\tau'_{b,t}=0.5\,\rho_w\,f'_w\,|U_{w,t}|\,U_{w,t} \qquad (1)$$

with: f'_w=grain-related wave friction factor, $U_{w,t}$=instantaneous orbital velocity at edge of wave boundary layer.

Basically, a detailed boundary layer model is required to compute the bed-shear stresses in strongly, asymmetric wave motion (saw-tooth waves). Figure 3 shows the bed-shear stresses in symmetric and asymmetric saw-tooth waves (strong forward leaning waves in asymmetric wave motion, U_{max}=1 m/s, T=5 s, $k_s=2.5d_{50}$) based on results from a boundary layer model including k-ε based turbulent shear stresses (Grasmeijer, 2004). It can be seen that the peak bed-shear stress increases by about 10% to 15% in asymmetric wave motion (second panel from top).

Nielsen (1992) has suggested a method to compute the instantaneous bed-shear stress under skewed wave motion including enhanced acceleration effects in asymmetric waves. This method includes the phase lead (φ_τ) of the bed-shear stress compared with the free-stream velocity.

The method of Nielsen (1992) for turbulent flow conditions reads, as:

$$\tau'_{b,t}=0.5\rho_w f'_w\,|[\cos(\varphi_\tau)\,(U_{w,t})+\omega^{-1}\sin(\varphi_\tau)(dU_w/dt)]|\,[\cos(\varphi_\tau)(U_{w,t})+\omega^{-1}\sin(\varphi_\tau)(dU_w/dt)] \qquad (2)$$

The time derivative can be evaluated as: $dU_w/dt= (U_{w,t+\Delta t} - U_{w,t-\Delta t})/(2\Delta t)$. In the case of a simple sinusoidal wave motion, Equation (2) yields a simple sinusoidal bed-shear stress shifted forward by the phase angle φ_τ. In the case of asymmetric wave motion the bed-shear stresses are enhanced during times of acceleration. For waves with saw-tooth type of asymmetry this leads to a dominant onshore shear stress and hence net onshore transport. This enhancement of the bed-shear stress from higher harmonics expresses the physical fact that high-frequency waves have thinner boundary layers and hence larger shear stresses. Wijetunge and Sleath (1998) have made velocity measurements using LDA in oscillatory flow in a wave tunnel to determine the phase lead effects. The phase lead of τ_{max} (with respect to free-stream velocity) is found to be about 45^o just above the non-moving bed and about 30^o at y=0 (initial bed) and about zero at 10 mm above the bed (near top of sheet flow layer).

The method of Nielsen (1992) has been used to compute the bed-shear stress under asymmetric waves described by $U=U_1\cos(\omega t)+U_2\cos(2\omega t)$. The data of an experiment of Ribberink et al. (2000) have been used as input data: U_{max}=1.45 m/s, U_{min}=-0.7 m/s, T=9 s, d_{50}=0.21 mm, d_{90}=0.32 mm, $q_{b,net}=108\ 10^{-6}$ m^2/s=0.29 kg/s/m. Figure 4 shows the instantaneous free-stream velocity and the dimensionless mobility (Shields) parameter

$\theta' = \tau'_{b,t}/((\rho_s-\rho_w)gd_{50})$ with $\tau'_{b,t}$ based on Equation (2) without phase lag and with phase lag. The friction factor is taken as f'_w=0.01. Computed results are shown for phase leads of 0, 10°, 25° and 40° degrees (Figure 4). The curves are shifted forward for phase lags (leads) of 10°, 25° and 40° degrees. The peak bed-shear stress increases with increasing phase lag. Using a simple bed-load transport formula, Nielsen and Callaghan (2003) show that the inclusion of the acceleration effects leads to a much better agreement of the computed net sand transport rate with measured values for a large-scale wave flume experiment. Wave-related streaming effects were found to be much less important. Herein, it is assumed that the method of Nielsen (1992) yields sufficiently accurate results of the instantaneous bed-shear stress in asymmetric wave motion.

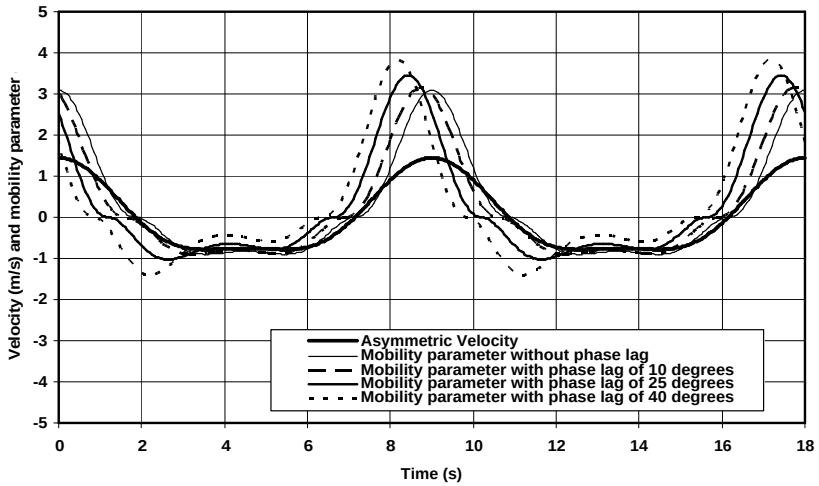

Fig. 4. Velocity and mobility (Shields) parameter as function of time; asymmetric velocity

BED FORM REGIME

As the value and direction of the net sediment transport is strongly related to the type of bed forms (ripples or flat bed), it is necessary to predict the type of bed forms and their effective bed roughness. Van Rijn (2006, 2007) has proposed a method to predict the effective bed roughness (k_s) of the bed forms in combined current and wave conditions.

CROSS-SHORE BED-LOAD TRANSPORT

It is assumed that the instantaneous bed-load transport rate (kg/s/m) is related to the instantaneous bed-shear stress, which is based on the instantaneous velocity vector (including both wave-related and current-related components) defined at a small height above the bed. The formula applied, reads as:

$$q_b = \gamma \rho_s d_{50} D_*^{-0.3} [\tau'_{b,cw}/\rho]^{0.5} [(\tau'_{b,cw} - \tau_{b,cr})/\tau_{b,cr}]^{\eta} \quad (3)$$

in which: $\tau'_{b,cw}$= instantaneous grain-related bed-shear stress due to both currents and waves= $0.5 \rho f'_{cw} (U_{\delta,cw})^2$; $U_{\delta,cw}$= instantaneous velocity due to currents and waves at edge of wave boundary layer; f'_{cw} = grain friction coefficient due to currents and waves= $\alpha\beta f'_c + (1-\alpha) f'_w$; f'_c = current-related grain friction coefficient, f'_w = wave-

related grain friction coefficient, α= coefficient related to relative strenght of wave and current motion, β= coefficient related to vertical structure of velocity profile, $\tau_{b,cr}$= critical bed-shear stress according to Shields, ρ_s= sediment density, ρ = fluid density, d_{50} = particle size, D_* = dimensionless particle size, γ= coefficient= 0.5, η= exponent= 1 (based on calibration by using measured data, see Van Rijn, 2006).
The net bed-load transport rate can be obtained by time-averaging (over the wave period T) of the instantaneous transport rate using a bed-load transport formula for steady flow (quasi-steady approach), as follows: $q_b = (1/T) \int q_{b,t}\, dt$ with $q_{b,t}$ = F(instantaneous hydrodynamic and sediment transport parameters).
Equation (3) is based on the assumption that the sediment particles respond instantaneously (quasi-steady) to the oscillatory fluid motion near the bed. The net transport rate will always be in the direction of the largest peak orbital velocity. This assumption is reasonably valid for the sheet flow regime with sediment particles larger than about 0.2 mm. According to Dohmen-Janssen (1999), the phase-lag effects can be very well represented by the parameter $P=\delta_s \omega / w_s$ with δ_s= thickness of sheet flow layer (order of 0.01 m), $\omega=2\pi/T$=angular frequency, T= wave period. Phase-lag effects are important for fine sediment, large peak orbital velocities and small wave periods (P>0.5). Dohmen-Janssen (1999) proposed to correct the bed-load transport rates based on quasi-steady expressions, using a correction factor dependent on the P-parameter. Thus: $q_{b,net}= r\, q_{b,net,\ steady}$ with $r=F(p)$=correction factor between 0 and 1, $q_{b,net,\ steady}$=net bed-load transport according to quasi-steady expression. Using this approach, the net bed-load transport rate will be reduced but the net transport rate can not be against the direction of the largest peak velocity, which may occur over a rippled bed.

CROSS-SHORE SUSPENDED LOAD TRANSPORT

Two methods to compute the cross-shore transport rates are herein explored on their ability to represent the cross-shore transport in a cross-shore profile model. (CROSMOR). Both models can deal with negative oscillatory suspended transport rates due to the presence of rippled beds.

Method of Houwman and Ruessink (1996)

The wave-related suspended transport can also be estimated by the approach introduced by Houwman and Ruessink (1996).
The wave-related suspended transport at level z is given by:

$$q_{s,w,z}=(1/T) \int_o^T \langle U_w C_w \rangle \qquad (4a)$$

Using: $C_w=k_1 / U_w^3 /$, it follows that:

$$q_{s,w,z}=(1/T) \int_o^T [k_1 U_w / U_w^3 / dt] \qquad (4b)$$

Using: $U_w=U_{on} \sin(\omega t)$ with $\omega=2\pi/T$ for $0<t<0.5T$ and $U_w=U_{off} \sin(\omega t)$ for $0.5T<t<T$, the time-averaged concentration is given by:

$$c_z=(k_1/(0.5T)) \int_o^{0.5T} / U_{on}^3 / \sin^3(\omega t) dt + (k_1/(0.5T)) \int_{0.5T}^T / U_{off}^3 / \sin^3(\omega t) dt =$$

$$=k_1(2/T)\,[U^3_{on}+U^3_{off}]\;{}_o\!\int^{0.5T}\;|\sin^3(\omega t)|\,dt \qquad (4c)$$

The k_1-coefficient of Equation (4c) is substituted in Equation (4b), resulting in:

$$q_{s,w,z}=(1/T)\;c\;{}_o\!\int^{T}\;[A^{-1}][U_w\,|U_w{}^3|\,dt] \qquad (4d)$$

with: $A= (2/T)\,[U^3_{on}+U^3_{off}]\;{}_o\!\int^{0.5T}\;|\sin^3(\omega t)|\,dt$
This yields:

$$q_{s,w,z}=\gamma\,[(U^4_{on}-U^4_{off})/(U^3_{on}+U^3_{off})]\;c \qquad (4e)$$

with: $\gamma=I_3/I_4$; $I_3=(1/T)\;{}_o\!\int^{0.5T}\;\sin^4(\omega t)dt$; $I_3=(2/T)\;{}_o\!\int^{0.5T}\;|\sin^3(\omega t)|\,dt$; the γ-value is $9\pi/64\cong0.44$.

The total wave-related suspended transport component in the near-bed region can be estimated, as follows:

$$q_{s,w}=\gamma f_P\,[(U_{on})^4-(U_{off})^4]/[(U_{on})^3+(U_{off})^3]\;\int c\,dz \qquad (5a)$$

with: $U_{on}=U_{\delta,f}$= near-bed peak orbital velocity in onshore direction (in wave direction) and $U_{off}=U_{\delta,b}$= near-bed peak orbital velocity in offshore direction (against wave direction), c= time-averaged concentration (integrated over the wave boundary layer) and γ= coefficient, f_P= function to include phase lag effects. Grasmeijer (2002) has determined the γ-coefficient by fitting of Equation (5a) to the measured wave-related transport rates, yielding values in the range of 0.1 to 0.2
As phase lag effects are related to the wave conditions, sand size and bed geometry (ripples), the f_p-function is supposed to be a complicated function of these parameters (yielding negative values for very fine sand).

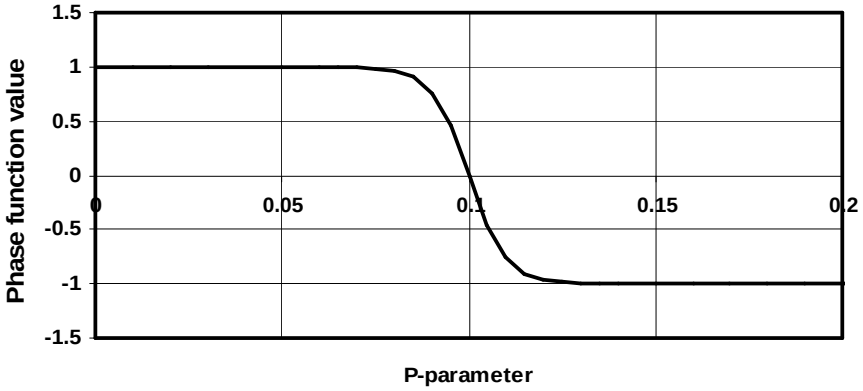

Fig. 5. Phase function of wave-related suspended transport

Assuming that the net suspended transport in onshore or in offshore direction is of the same order of magnitude (maximum values are about +0.02 or -0.02 kg/m/s), the phase

function is herein assumed to vary between +1 (fully onshore-directed) and -1 (fully offshore-directed). The phase function is tentatively described by (see Figure 5):

$$f_P = -\tanh[100(P-P_{cr})] \quad (5b)$$

with: $P=k_{s,w,r}/(w_s T_p)$, $k_{s,w,r}$=wave-related bed roughness height (estimate of ripple height), w_s= settling velocity of bed material, T_p=peak wave period, P_{cr}=0.1, yielding onshore transport for $P<P_{cr}$ and offshore transport for $P>P_{cr}$.
Simulation of the wave-related suspended transport according to Equation (5) requires computation of the time-averaged sand concentration profile and integration of the time-averaged sand concentration profile in vertical direction. Herein, the integration is taken over a near-bed layer with a thickness equal to about 10 times the thickness of the wave boundary layer (about 0.25 to 0.5 m), assuming that the suspended sand concentrations above this layer are not much effected by the high-frequency wave motion with periods in the range of T= 5 to 10 s. This assumption is satisfied if the fall time of a suspended sand particle over a distance of 0.25 to 0.5 m is much larger than the wave period ($T_{fall}= 0.5/w_s$ yielding about 25 s for d= 0.2 mm with w_s= 0.02 m/s). Furthermore, the data of the Deltaflume (Grasmeijer, 2002) show that most of the wave-related suspended transport occurs in the near-bed layer with a thickness of about 0.5 m (10 to 20 times the ripple height).

Method of van der Werf (2006)
Using a large amount of net transport data from oscillatory flow tunnel experiments, Van der Werf (2006) has developed a relatively simple model for net transport (mainly suspended sediments) in oscillatory flow over a rippled bed following the ideas of Dibajnia and Watanabe (1992). It is based on the division of the wave motion into an onshore and an offshore directed half wave-cycle. The net transport is the sum of both onshore and offshore quantities, as follows:

$$q_t = 6.75\,[Y/|Y|][|Y|^{0.64}][(s-1)g(d_{50})^3]^{0.5} \quad (6a)$$
$$Y = [U_c T_c\{(\Omega_{c1})^3+(\Omega_{t2})^3\} - U_t T_t\{(\Omega_{t1})^3+(\Omega_{c2})^3\}]/[(U_c+U_t)T] \quad (6b)$$

with:
q_t= net sand transport (m^2/s)
$P_w=\Delta_r/d_{50}$=vortex suspension parameter
$P_{w,cr}$=35
Δ_r=ripple height (measured or predicted); herein $k_{s,w,r}=\Delta_r$
$f'_w = exp(-6+5.2(A_w/2.5d_{50})^{-0.19})$=grain-related friction factor
A_w= orbital excursion amplitude
U_c= representative peak wave crest velocity (onshore-directed, positive value)
U_t= representative peak wave trough velocity (offshore-directed, positive value)
T_c= duration of wave crest phase
T_t=duration of wave trough phase
$T = T_c + T_t$=wave period
if $P_w \leq P_{w,cr}$

$\Omega_{c1}=0.5\, f'_w\, (U_c)^2/((s-1)gd_{50})$=onshore-entrained and onshore-directed transport
$\Omega_{c2}=0$
$\Omega_{t1}=0.5\, f'_w\, (U_t)^2/((s-1)gd_{50})$= offshore-entrained and offshore-directed transport
$\Omega_{t2}=0$
if $P_w>P_{w,cr}$
$\Omega_{c1}=(P_w/P_{w,cr})0.5\, f'_w\, (U_c)^2/((s-1)gd_{50})$=onshore-entrained and onshore-directed tr.
$\Omega_{c2}=((P_w-P_{w,cr})/P_w)\ 0.5\, f'_w\, (U_c)^2/((s-1)gd_{50})$=onshore-entrained and offshore-directed
$\Omega_{t1}=(P_w/P_{w,cr})0.5\, f'_w\, (U_t)^2/((s-1)gd_{50})$= onshore-entrained and onshore-directed tr.
$\Omega_{t2}=((P_w-P_{w,cr})/P_w)\ 0.5\, f'_w\, (U_t)^2/((s-1)gd_{50})$=offshore-entrained and onshore-directed

The model has been developed for wave-only flows and is valid in the rippled bed regime only. Currently, a new practical model for net sand transport induced by non-breaking waves and currents is being developed within the SANTOSS research project (see the Coastal Sediments 2007 paper by Van der Werf et al.).

If P_w is larger than $P_{w,cr}$, the total amount of entrained sediment during a wave cycle should be divided in two parts: one part transported as bed load and near-bed suspended load during the same half wave cycle and a second part transported as suspended load (in the opposite direction) during the next half cycle. Net transport rates become negative (offshore-directed) when more sand is transported during the offshore half cycle than during the onshore half cycle. This occurs when P_w is approximately twice as large as $P_{w,cr}$. If P_w is smaller than $P_{w,cr}$, there is no sediment interaction between the two half wave cycles, transport takes place only very close to the bed, entrained and transported in the direction of the peak velocity.

Cross-shore morphology

Two tests from the LIP experiments (Sánchez-Arcilla, 1995) have been used to study the effect of wave-related transport on the nearshore morphology using the process-based CROSMOR profile model. Test1B simulates a storm condition with a breaker bar in the surf zone moving in offshore direction (offshore event). Test 1C simulates a typical swell condition (post-storm) with a breaker bar in the surf zone moving in onshore direction (onshore event). The bed material consists of sand with d_{10}=150, d_{50}=200, d_{90}=400 μm. The offshore water depth (h_o) to still water level is 4.1 m in all tests. The model is run in standard mode with all cross-shore wave, flow and sand transport processes included (Van Rijn 2006, 2007). The effect of the wave-induced fluid acceleration in asymmetric waves on the bed-shear stress and hence on the bed-load transport has been included. The computed wave-related net sand transport rates (due to wave asymmetry) are found to be in onshore direction, when the phase lag effects on sand transport processes are excluded. The wave-breaking induced undertow causes offshore-directed sand transport rates. Bed level changes depend on the gradients of the balance of these two transport components.

Test1B

Figure 6A,B shows the measured and computed wave heights, undertow velocities and peak orbital velocities for Test 1B. Computed wave heights are rather good. The

computed undertow velocites are in good agreement with the measured values with exception in the region close to the waterline. Computed peak orbital velocites are in good agreement with measured values. Measured data in the region close to the waterline are not available.

Figures 7A,B show the measured and computed bed levels after 18 hours using the transport method of Van Rijn. The generation and migration of the outward breaker bar is simulated rather well for Test 1B. When only the undertow transport component is taken into account, the simulated bar is in its most outward position (Fig. 7A). Conversely, when only the onshore wave-related transport components are taken into account, the simulated bar is in its most inward position (Fig. 7A). The observed bar behaviour is slightly better simulated if the acceleration effects based on the method of Nielsen are included (Figure 7B). Fluid acceleration effects do not seem to be very important for breaking wave conditions, because wave velocity skewness is suppressed in breaking wave conditions. Inclusion of phase lag effects has not much influence on the computed bed levels. The model also predicts an inner bar with sand eroded from the beach for Test 1B; the measured bed profile does not show this behaviour. Thus, the physics close to the shore are not simulated properly. Both the undertow velocity and the wave asymmetry have to be improved significantly.

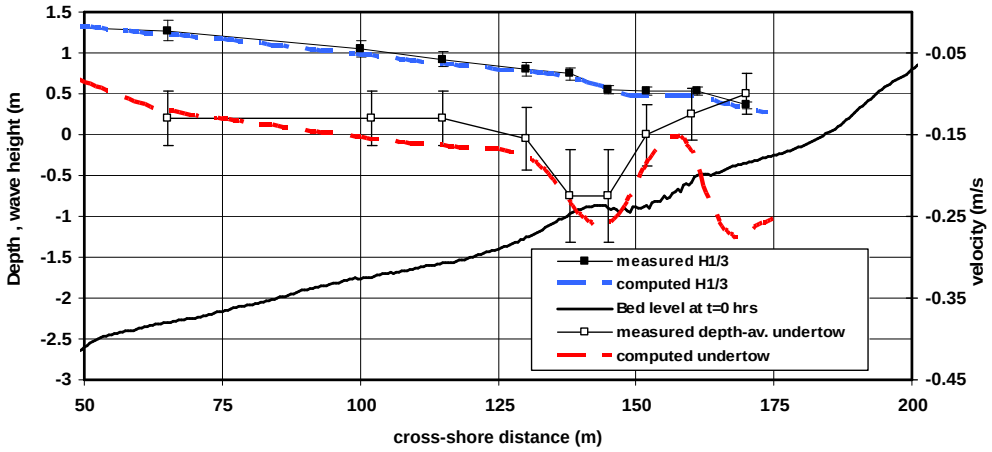

Fig. 6A. Measured and computed wave height and undertow for Test 1B

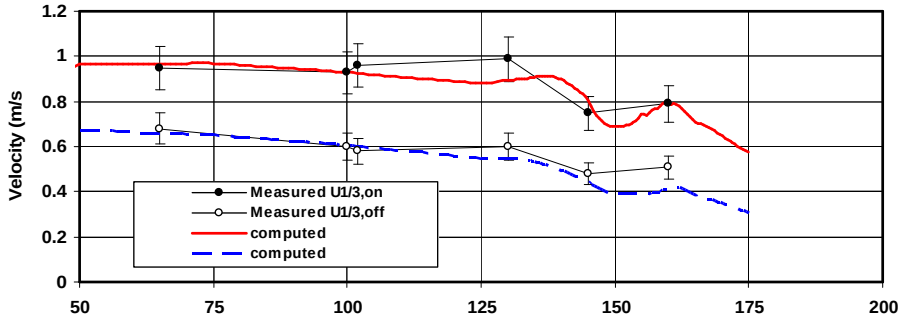

Fig. 6B. Measured and computed peak orbital velocities for Test 1B

Figure 7C shows measured and computed bed levels using the transport method of Van

der Werf (Equation 6). This method yields transport values of the right order of magnitude, but it can not yet simulate the undertow transport component. The offshore bar migration is much too small excluding the undertow transport component and much too large including the undertow transport component (based on the Van Rijn method).

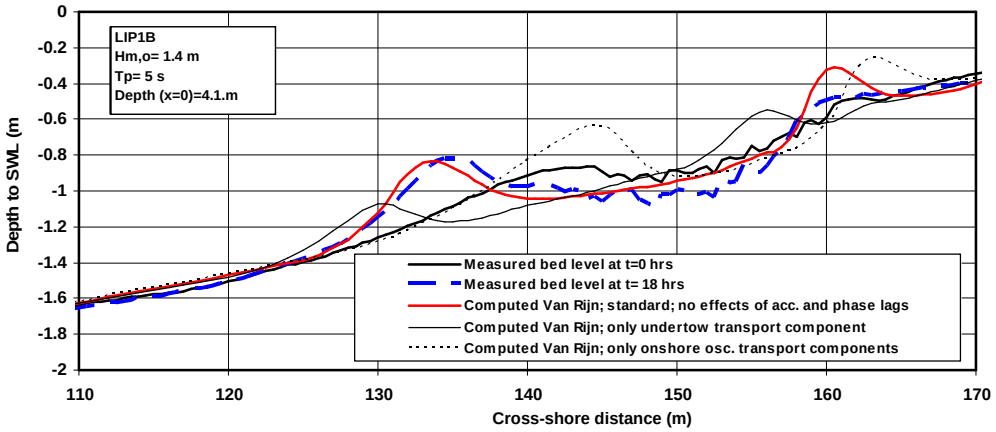

Fig. 7A. Measured and computed bed levels for Test 1B; method Van Rijn

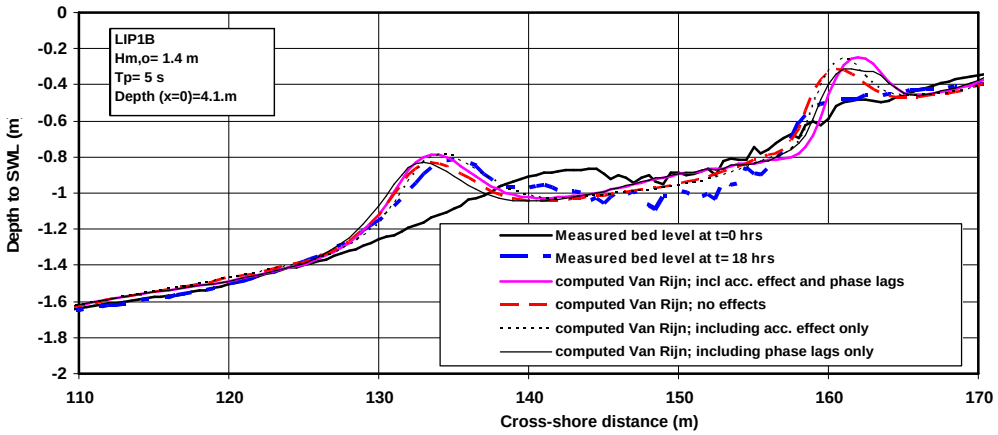

Fig. 7B. Measured and computed bed levels for Test 1B; method Van Rijn

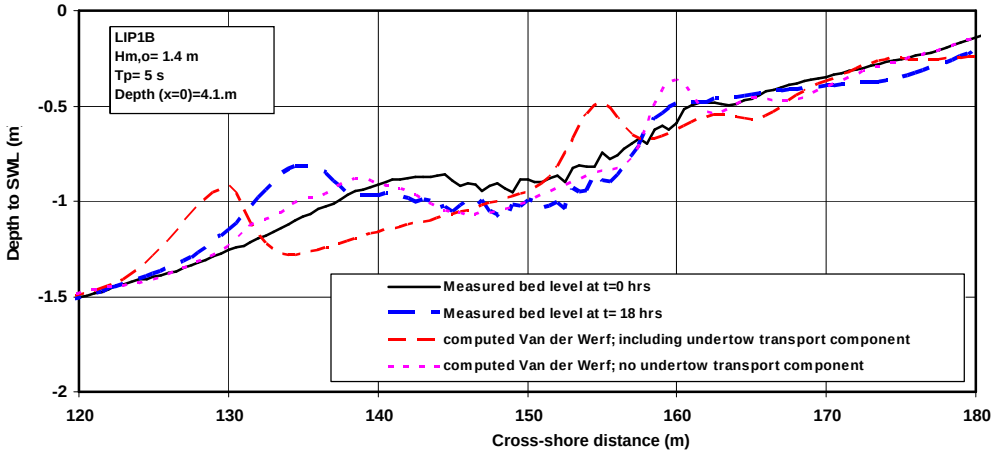

Fig. 7C. Measured and computed bed levels for Test 1B; method Van der Werf

Test 1C

Figure 8 shows that the standard model of Van Rijn also yields onshore bar migration, but the onshore migration is much too small. Inclusion of the acceleration effect on the bed-load transport improves the prediction. Inclusion of phase lag effects has almost no effect, which means that phase function predicts onshore-directed suspended load transport in agreement with the observed onshore bar migration. Probably, the observed bed ripples are not steep enough (under irregular waves) to generate strong vortex motions with phase lags between sediment concentration and orbital velocity and hence offshore-directed transport. The transport method of Van der Werf (Equation 6) produces similar trends (not shown) as for Test 1B; the transport rates are of the right order of magnitude. The bar moves onshore neglecting the undertow transport component, but it moves offshore including the undertow transport component.

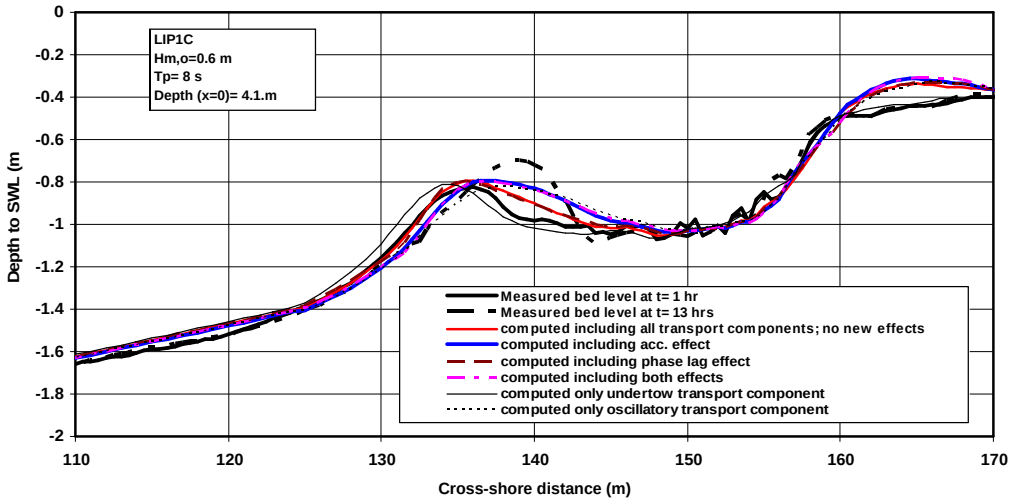

Fig. 8. Measured and computed bed levels for Test 1C; method Van Rijn

CONCLUSIONS

Summarizing, the model runs show that the sediment transport model of Van Rijn can simulate the qualitative aspects of the outer surf zone dynamics reasonably well. Fluid acceleration effects on bed-shear stress and hence on sand transport appear to be important for low wave conditions, but not for storm conditions (breaking waves). It is most important to model the onshore-directed wave asymmetry transport and the offshore-directed transport by the undertow correctly. Phase lag effects influencing the wave-related transport do not seem to be very important under irregular waves over a sand bed of about 0.2 mm. Future work will be focussed on improvement of the wave skewness and asymmetry close to the shore. The transport model of Van der Werf (2006) can represent the trends observed in the laboratory experiments. However, the validity of this model is limited to wave-only flows over rippled beds. Currently, the model is being extended to also cover the flat-bed/sheet-flow regime and to include the current-related related transport.

REFERENCES

Dibajnia M., and Watanabe, W. 1992. Sheet-flow under non-linear waves and currents. Proc. 23rd ICCE, Venice, Italy, pp. 2015-2025.

Doering, J.C. and A.J. Bowen, 1995. Parameterization of orbital velocity asymmetries of shoaling and breaking waves using bispectral analysis. Coastal Eng., 26, 15-33.

Dohmen-Janssen, C.M., 1999. Grain size influence on sediment transport in oscillatory sheet flow: phase lags and mobile-bed effects. Doctoral Thesis, Delft University of Technology, Delft, The Netherlands, 246 pp.

Grasmeijer, B.T., 2002. Process-based cross-shore modelling of barrred beaches. Doctoral Thesis, Dep. of Physical Geography, Univ. Utrecht, The Netherlands.

Grasmeijer, B.T., 2004. Personal communication.

Henderson, S.M., J.S. Allen, and P.A. Newberger, 2004. Nearshore sandbar migration predicted by an eddy-diffusive boundary layer model. Journal of Geophysical Research, 109, C06024, doi:10.1029/2003JC002137.

Hoefel, F. and S. Elgar, 2003. Wave-Induced Sediment Transport and Sandbar Migration. Science, 299, 1885-1887.

Houwman, K.T. and Ruessink, B.G., 1996. Sediment transport in the vicinity of the shoreface nourishment of Terschelling. University of Utrecht, The Netherlands.

Hsu, T.J., S. Elgar and R.T. Guza, 2006. Wave-induced sediment transport and onshore sandbar migration. Coastal Engineering, 53, 817-824.

Isobe, M. and Horikawa, K., 1982. Study on water particle velocities of shoaling and breaking waves. Coastal Engineering in Japan, Vol. 25.

Nielsen, P., 1992. Coastal Bottom Boundary Layers and Sediment Transport. Advanced series on Ocean Engineering, volume 4. World Scientific, Singapore, 324 p.

Nielsen, P. and Callaghan, D.P., 2003. Shear stress and sediment transport calculations for sheet flow under waves. Coastal Engineering, Vol. 47, p. 347-354.

Ribberink, J.S., 1998. Bed-load transport for steady flows and unsteady oscillatory flows. Coastal Eng., Vol. 34, No. 1-2, p. 59-82.

Ribberink, J.S., Dohmen-Janssen, C.M., Hanes, D.M., McLean, S.R. and Vincent, C., 2000. Near-bed transport mechanisms under waves; a large-scale flume experiment. 27th ICCE, Sydney, Australia.

Sánchez-Arcilla, A. et al., 1994. The Delta Flume experiment 1993. Proc. Coastal Dynamics, UPC, Barcelona, p. 488-502

Van der Werf, J.J., 2006. Sand transport over rippled beds in oscillatory flow. Doctoral Thesis, Department of Civil Engineering, University of Twente, The Netherlands.

Van der Werf, J.J., Ribberink, J.S. and O'Donoghue, T. Development of a new practical model for sand transport induced by non-breaking waves and currents. Paper presented at Coastal Sediments 2007.

Van Rijn, L.C., 2006. Principles of sediment transport in rivers, estuaries and coastal seas. Part 2 Supplement/Update. Aqua Publications (www.aquapublications.nl)

Van Rijn, L.C., 2007. A unified view of sediment transport by currents and waves; Parts 1 to 4. Accepted by Journal of Hydraulic Engineering, ASCE (in Press)

Wijetunge, J.J. and Sleath, J.F.A., 1998. Effects of sediment transport on bed friction and turbulence. Journal of Waterway, Port, Coastal and Ocean Engineering, Vol. 124, No. 4, p. 172-178.